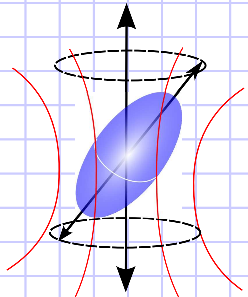

Çekirdek spinlerinde sıkıştırılmış ve Schrödinger kedisi durumları

Ceyhun Bulutay
Fizik Bölümü, Bilkent Üniversitesi, Ankara
3 February 2017

Teşekkürler:

- Ataç İmamoğlu (ETH)
- Tomáš Opatrný (Olomouc)
- QuTiP: The Quantum Toolbox in Python
- TÜBİTAK, Project No. 114F409

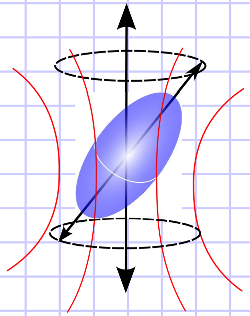

Squeezed and Schrödinger cat states with quadrupolar nuclear spins

Ceyhun Bulutay
Fizik Bölümü, Bilkent Üniversitesi, Ankara
3 February 2017

Acknowledgements:

- Ataç İmamoğlu (ETH)
- Tomáš Opatrný (Olomouc)
- QuTiP: The Quantum Toolbox in Python
- TÜBİTAK, Project No. 114F409

Outline

- Basics on Nuclear Spins
- Spin Squeezing via Quadrupole Interaction
- Cat States: Generation & Stabilization
- Timescales & Decoherence
- Discussion & Conclusions

Basics on Nuclear Spins

Nuclear Spin

- Each nuclear state is characterized by a unique "spin" quantum number I, representing the total angular momentum (orbital+intrinsic) of all the nucleons, $\vec{I} = \sum_{i=1}^{A} \vec{\ell}_i + \vec{s}_i$
- I : integer/half-integer based on nucleon number A : even/odd
- Predicting even the ground state nuclear spin not an easy feat: low-energy QCD
- Nevertheless, from experiment we know much about them

Rules that apply to ground state nuclear spins:

- N: # neutrons, Z: # protons, $A = Z + N$: # nucleons
- If N and Z are both even, $I = 0$ (based on pairing), eg., ${}^{12}_{6}C_6$, ${}^{28}_{14}Si_{14}$
  NB: $I = 0$ nuclei are NMR-silent
- If N and Z are both odd, I is full integer
  eg., ${}^{14}_{7}N_7 \Rightarrow I = 1$, ${}^{10}_{5}B_5 \Rightarrow I = 3$

Electrostatic Energy: Multipole Expansion

The electrostatic energy of a charge distribution $\rho(\vec{r})$ (here, nuclear charge) placed in an external field (here, due to crystal potential, V)

$$W = \int d\vec{r}\rho(\vec{r})V(\vec{r}),$$

$$V(\vec{r}) = V(0) + \sum_\alpha x_\alpha \frac{\partial V}{\partial x_\alpha}(0) + \frac{1}{2!}\sum_{\alpha,\beta} x_\alpha x_\beta \frac{\partial^2 V}{\partial x_\alpha \partial x_\beta}(0) + \cdots$$

$$W = \underbrace{qV(0)}_{\text{monopole}} \underbrace{-\vec{p}\cdot\vec{E}(0)}_{\text{dipole}} \underbrace{-\frac{1}{6}\sum_{i,j} Q_{ij}\frac{\partial E_i}{\partial x_j}(0)}_{\text{quadrupole}} + \cdots$$

Nuclear wavefunction has definite parity $\Longrightarrow$ odd moments vanish: no dipole/octopole, ...

N. Ramsey, *Nuclear Moments*, Wiley, 1953, pg. 24.

Nuclear Electric Quadrupole Moment

$$eQ = \int d\vec{r}\rho(r,z)\,(3z^2 - r^2)$$

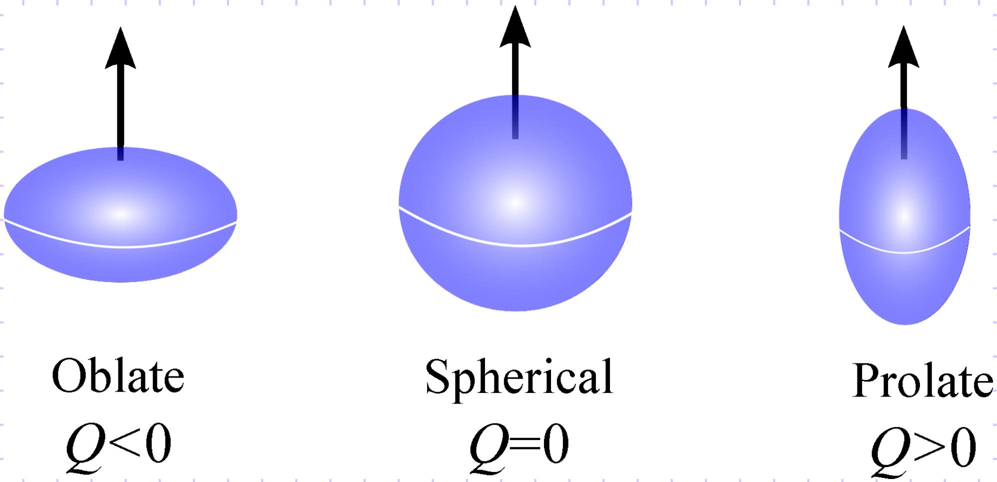

- Nuclei with I=0 and 1/2 have spherical charge distribution ⇒ no quadrupolar moment
  - Spherical nuclei: $Q = 0$, e.g., $I = 0$: ^{28}Si, ^{12}C; $I = 1/2$: ^{29}Si, ^{13}C
- Nuclei with $I \geq$1 are quadrupolar
  - Oblate nuclei: $Q < 0$, e.g., Li, Cu, V, Sc
  - Prolate nuclei: $Q > 0$, e.g., Al, Ga, As, In
- Spin quantization axis conveniently chosen to be along major EFG axis (Z)

Energetic Drive for Quadrupolar Alignment

Consider a prolate nucleus ($Q > 0$) placed at a point where $E_{tot} = 0$ but for two different field gradients:

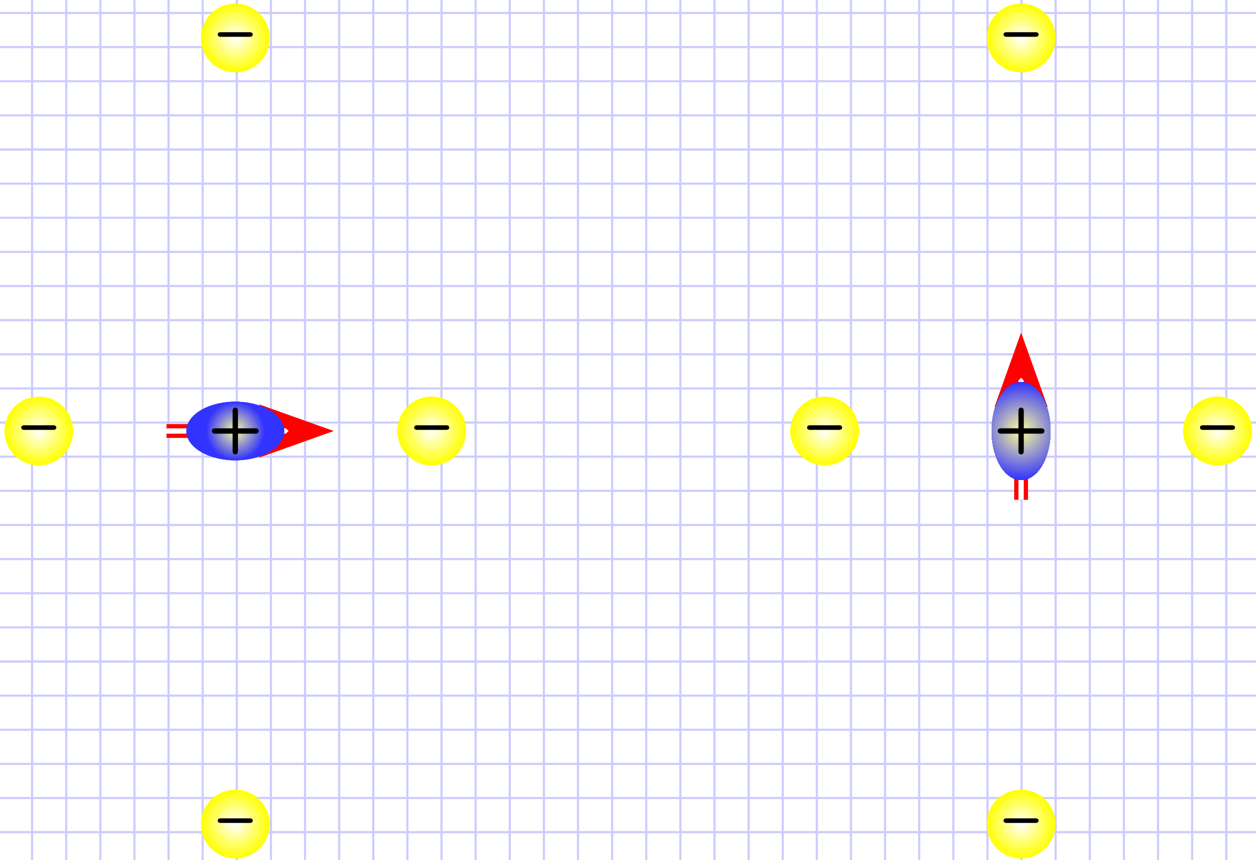

Energetic Drive for Quadrupolar Alignment

Consider a prolate nucleus ($Q > 0$) placed at a point where $E_{tot} = 0$ but for two different field gradients:

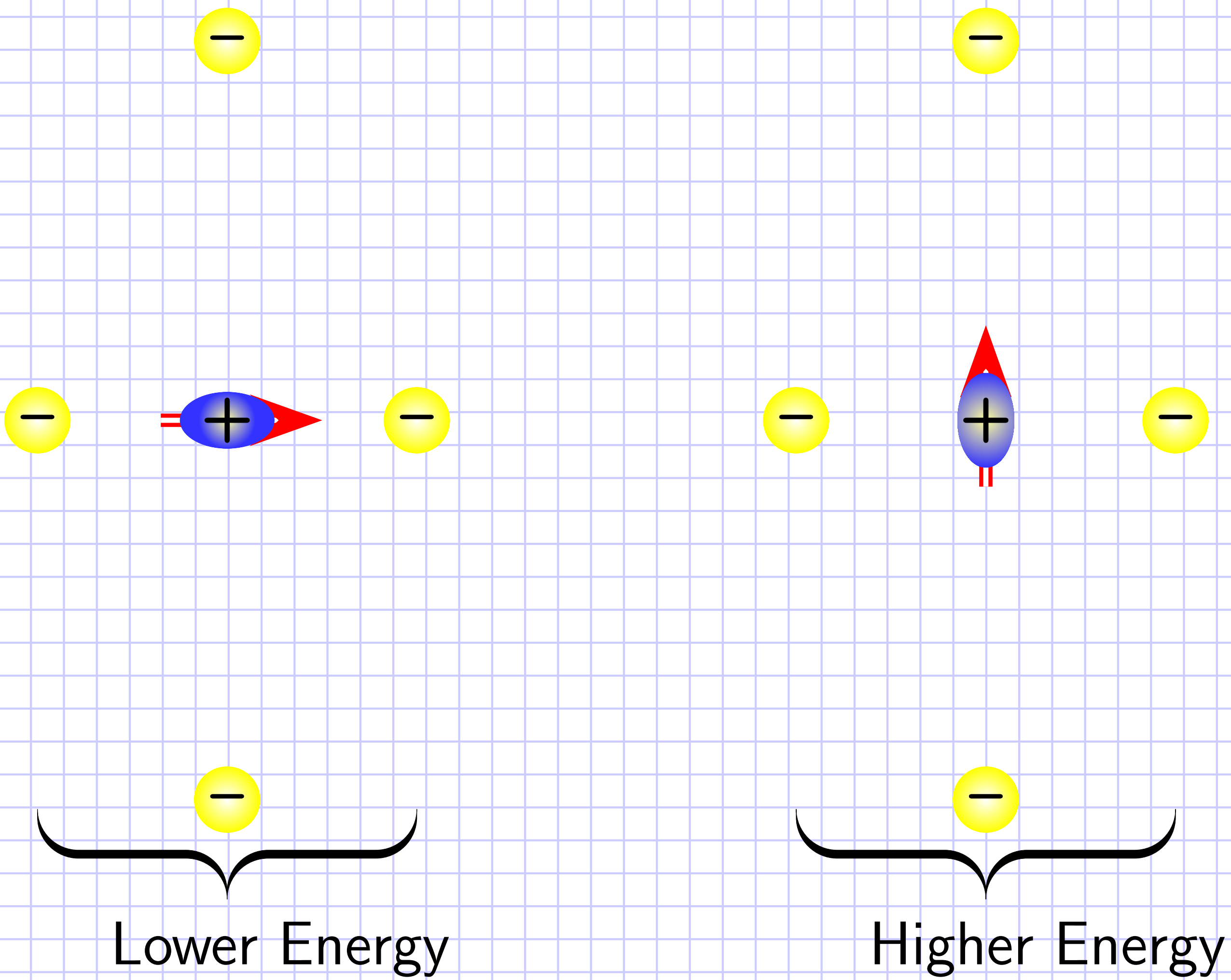

Origin of Degeneracy in Quadrupolar Spectra

The electrostatic energy of a cylindrical charge distribution is invariant within a quadrupolar field when reversed, unlike the Zeeman effect

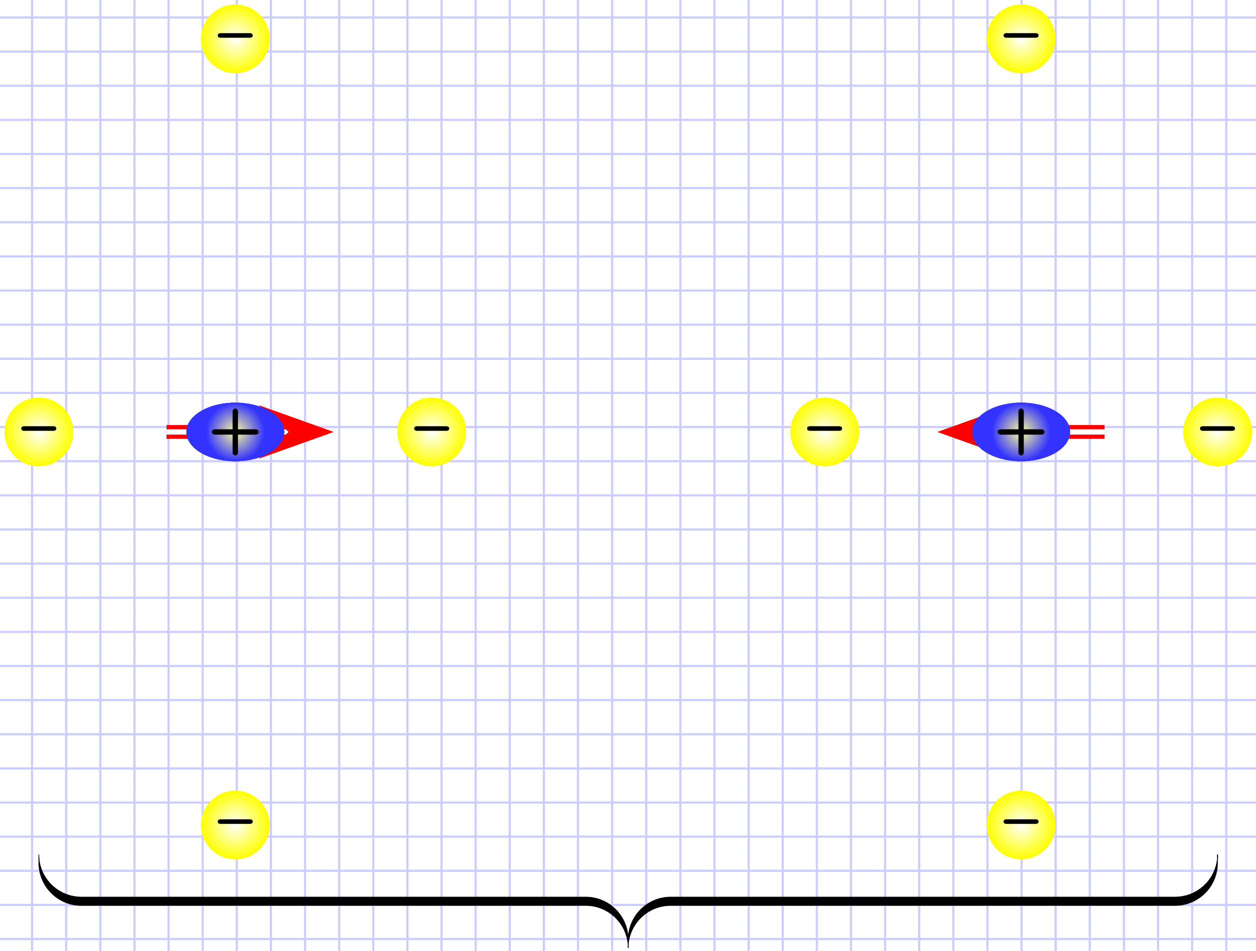

will lead to $\pm m$ degeneracy

Nuclear Spin Quadrupole Hamiltonian

In crystallographic coordinates and in Voigt notation:

EFG elastic strain tensor

$$V_{ij} \equiv \frac{\partial^2 V}{\partial x_i \partial x_j} \to V_{\mu} = \sum_{\nu=1}^{6} S_{\mu\nu} \epsilon_{\nu}$$

$$\left. \begin{array}{l} V_{zz} = S_{11}\left[\epsilon_{zz} - \frac{1}{2}\left(\epsilon_{xx} + \epsilon_{yy}\right)\right] = S_{11}\epsilon_B \,, \\ V_{xy} = V_{yx} = 2S_{44}\epsilon_{xy} \end{array} \right\} \text{ \& cyc. perm's.}$$

In EFG principal axes (XYZ), Quadrupole Hamiltonian:

$$\mathcal{H}_Q = \frac{e^2 q Q}{4I(2I-1)}\left[3\mathcal{I}_Z^2 - \mathcal{I}^2 + \eta \frac{\mathcal{I}_+^2 + \mathcal{I}_-^2}{2}\right] ,$$

EFG Axes

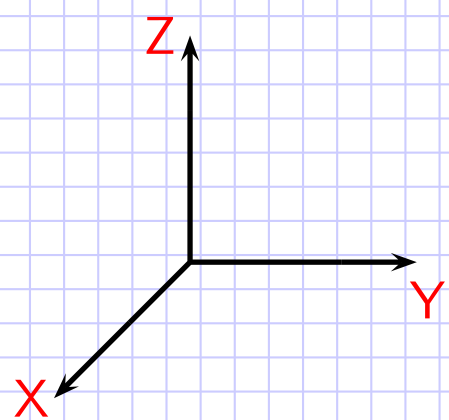

where $\left\{ \begin{array}{ll} eq \equiv V_{ZZ} , & \text{field gradient} \\ \eta \equiv \frac{V_{XX} - V_{YY}}{V_{ZZ}} , & \text{biaxiality} \end{array} \right. .$

$$|V_{zz}| \geq |V_{yy}| \geq |V_{xx}|$$

Nuclear Spin Quadrupole Hamiltonian

In crystallographic coordinates and in Voigt notation:

EFG elastic strain tensor

$$V_{ij} \equiv \frac{\partial^2 V}{\partial x_i \partial x_j} \to V_\mu = \sum_{\nu=1}^{6} S_{\mu\nu}\epsilon_\nu$$

$$\left.\begin{array}{l} V_{zz} = S_{11}\left[\epsilon_{zz} - \frac{1}{2}\left(\epsilon_{xx} + \epsilon_{yy}\right)\right] = S_{11}\epsilon_B\,, \\ V_{xy} = V_{yx} = 2S_{44}\epsilon_{xy} \end{array}\right\} \text{ \& cyc. perm's.}$$

In EFG principal axes (*XYZ*), Quadrupole Hamiltonian:

$$\mathcal{H}_Q \quad = \quad \frac{e^2 qQ}{4I(2I-1)}\left[3\mathcal{I}_Z^2 - \mathcal{I}^2 + \eta\frac{\mathcal{I}_+^2 + \mathcal{I}_-^2}{2}\right],$$

where $\left\{\begin{array}{ll} eq \equiv V_{ZZ}, & \text{field gradient} \\ \eta \equiv \frac{V_{XX}-V_{YY}}{V_{ZZ}}, & \text{biaxiality} \end{array}\right.$.

$$|V_{zz}| \geq |V_{yy}| \geq |V_{xx}|$$

EFG Axes/Bloch Sphere

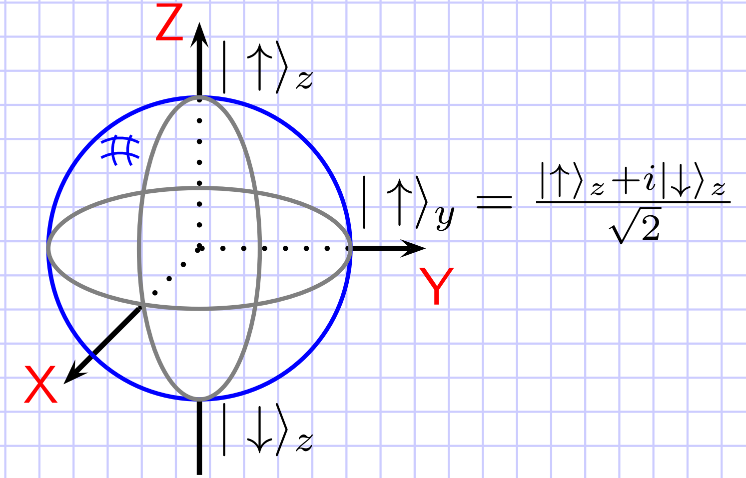

Spin Squeezing via Quadrupole Interaction

Quadrupole Interaction vs Squeezing Schemes

$$\hat{H}_Q = \frac{e^2 qQ}{4I(2I-1)}\left[3\hat{I}_z^{\,2} - \hat{I}^2 + \eta\frac{\hat{I}_+^2+\hat{I}_-^2}{2}\right];$$

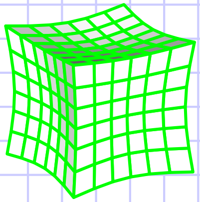

$\eta \equiv \frac{V_{XX}-V_{YY}}{V_{ZZ}}$ (biaxiality), $1 \geq \eta \geq 0$

All native twisting options: One-Axis / Mixed-Axis / Two-Axis

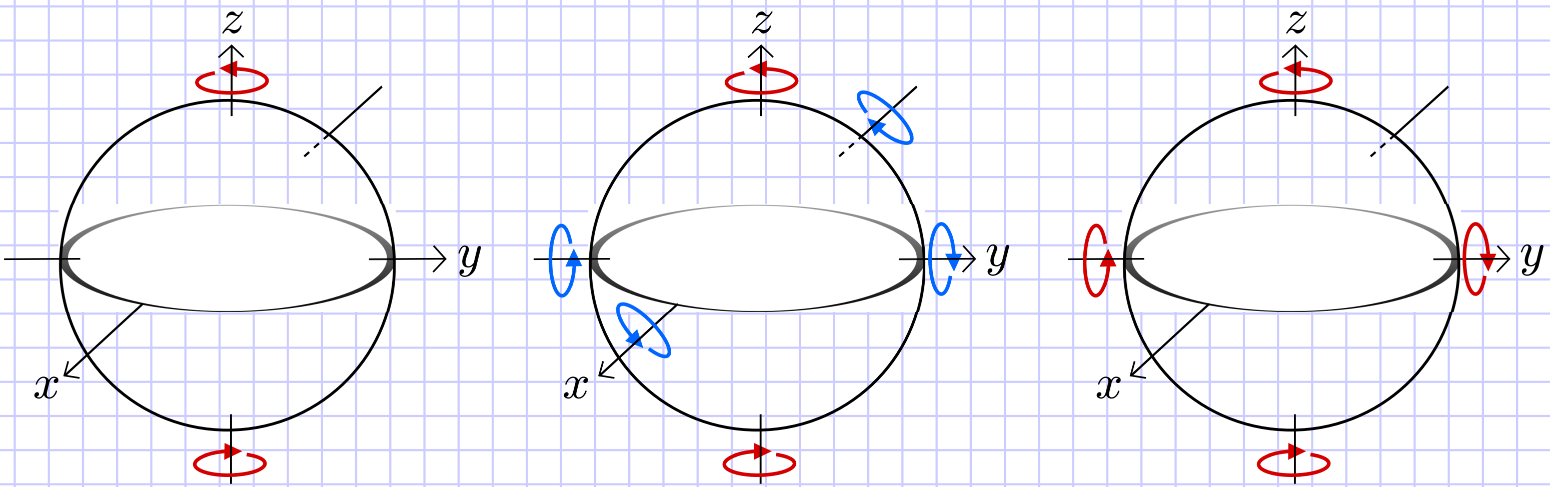

$\eta=0$	$0<\eta<1$	$\eta=1$
$\propto \hat{I}_z^2$	$\propto 3\hat{I}_z^2 + \eta(\hat{I}_x^2 - \hat{I}_y^2)$	$\propto (\hat{I}_z^2 - \hat{I}_y^2)$

Y. Aksu Korkmaz and CB, Phys. Rev. A **93**, 013812 (2016)

Stages of Squeezing

One-axis Twisting

$I = 9/2$, $|CSS\rangle = |X\rangle$, $\eta = 0$

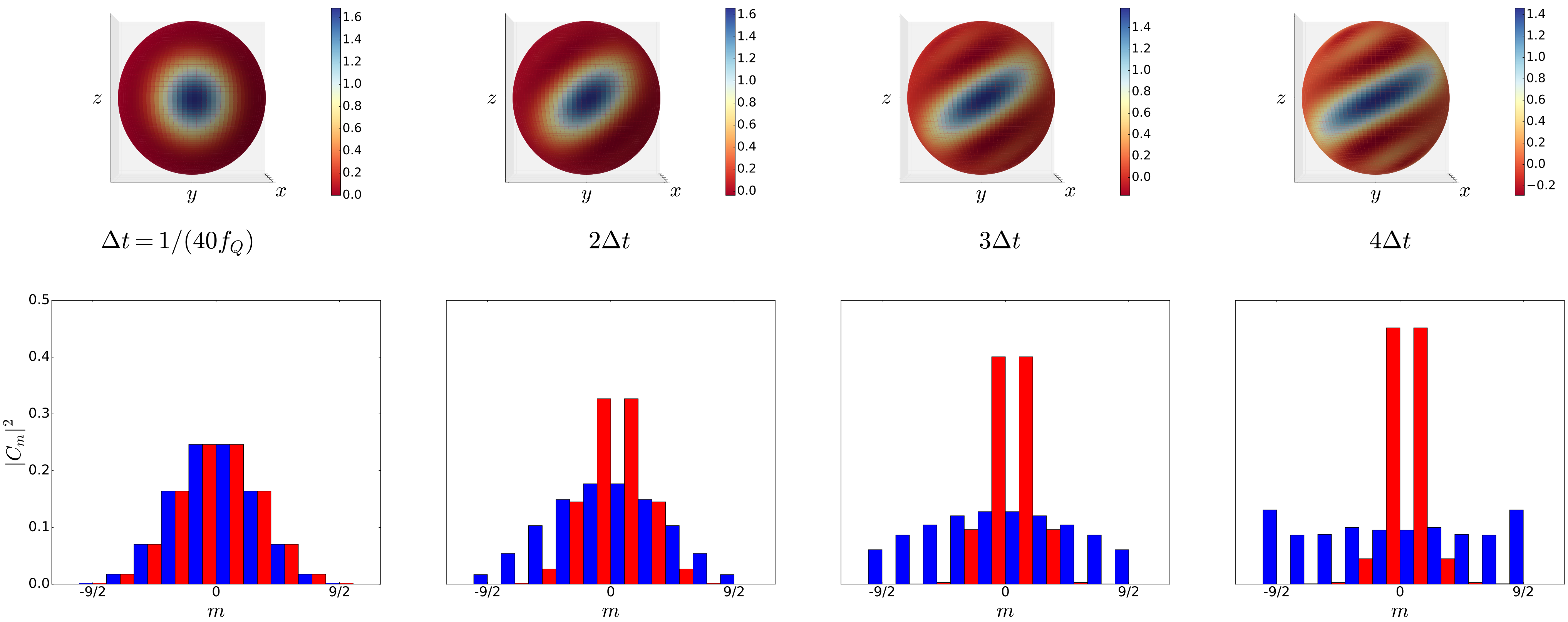

Squeezing progression . . .

Stages of Squeezing

One-axis Twisting

$I = 9/2$, $|CSS\rangle = |X\rangle$, $\eta = 0$

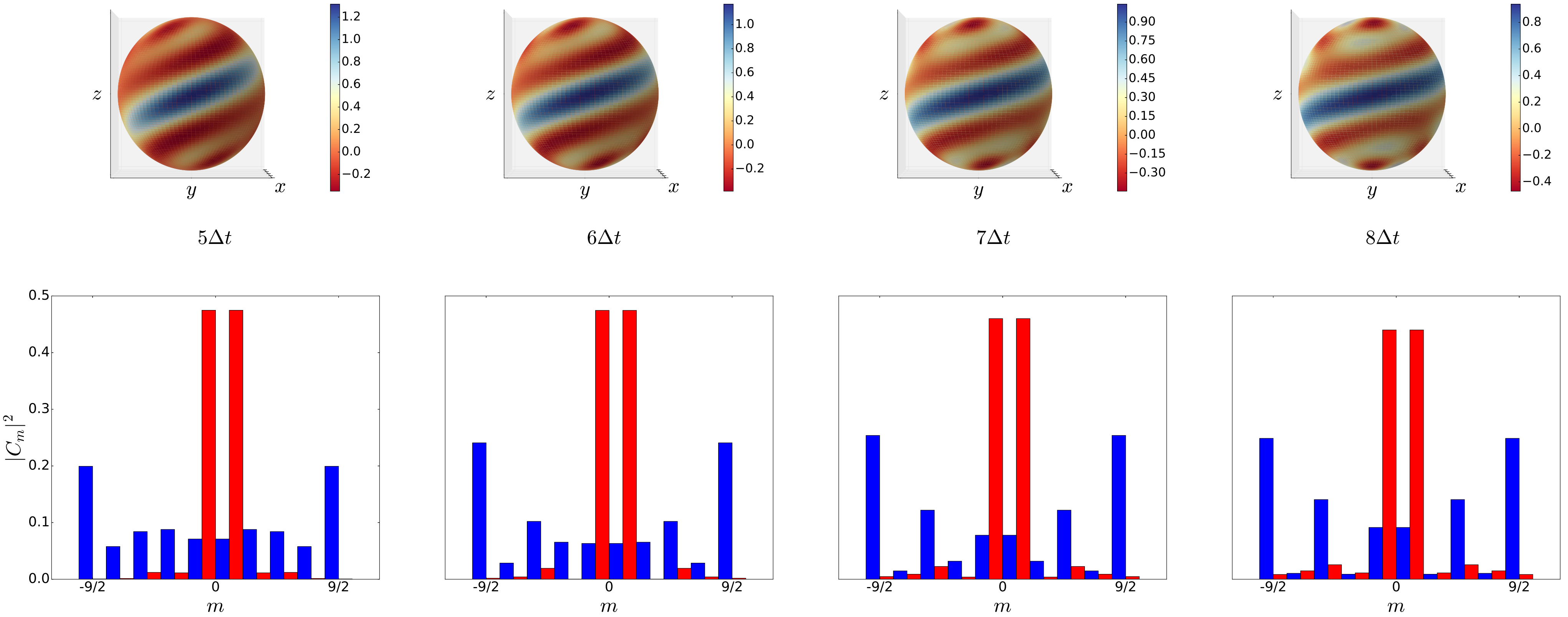

Anti-squeezing progression . . .

Stages of Squeezing

Two-axis Countertwisting

$I = 9/2$, $|CSS\rangle = |X\rangle$, $\eta = 1.0$

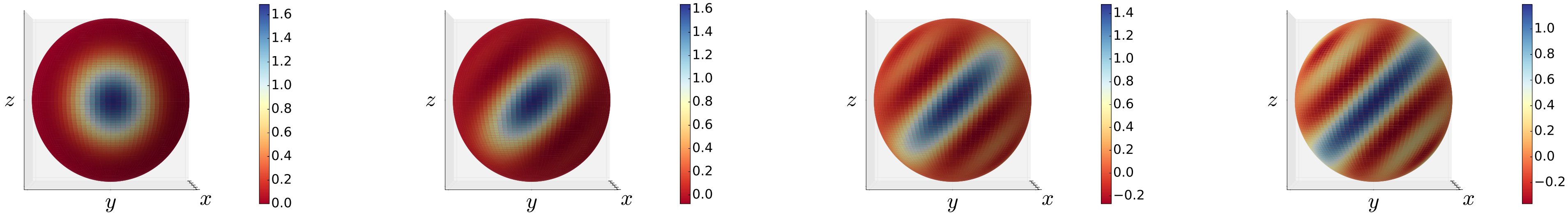

$\Delta t = 1/(40 f_Q)$ $2\Delta t$ $3\Delta t$ $4\Delta t$

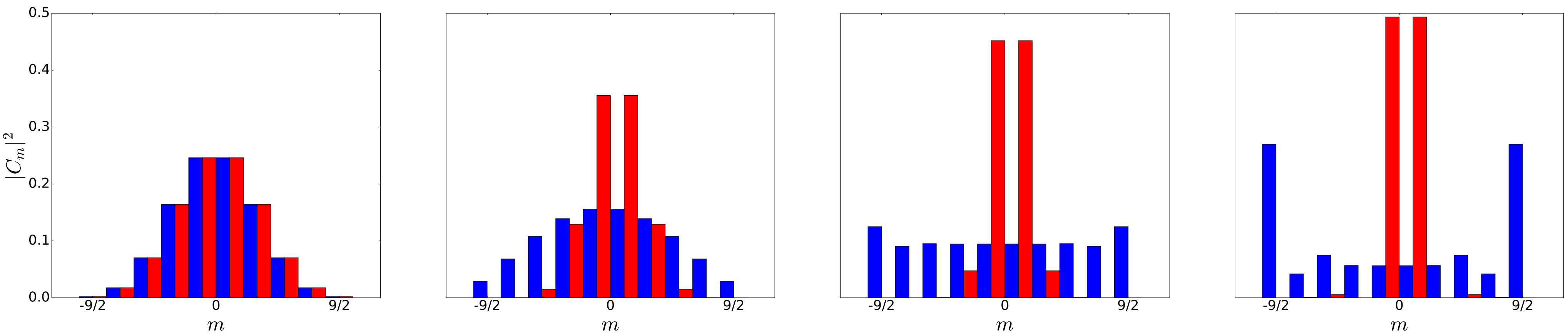

Squeezing progression . . .

Stages of Squeezing

Two-axis Countertwisting

$I = 9/2$, $|CSS\rangle = |X\rangle$, $\eta = 1.0$

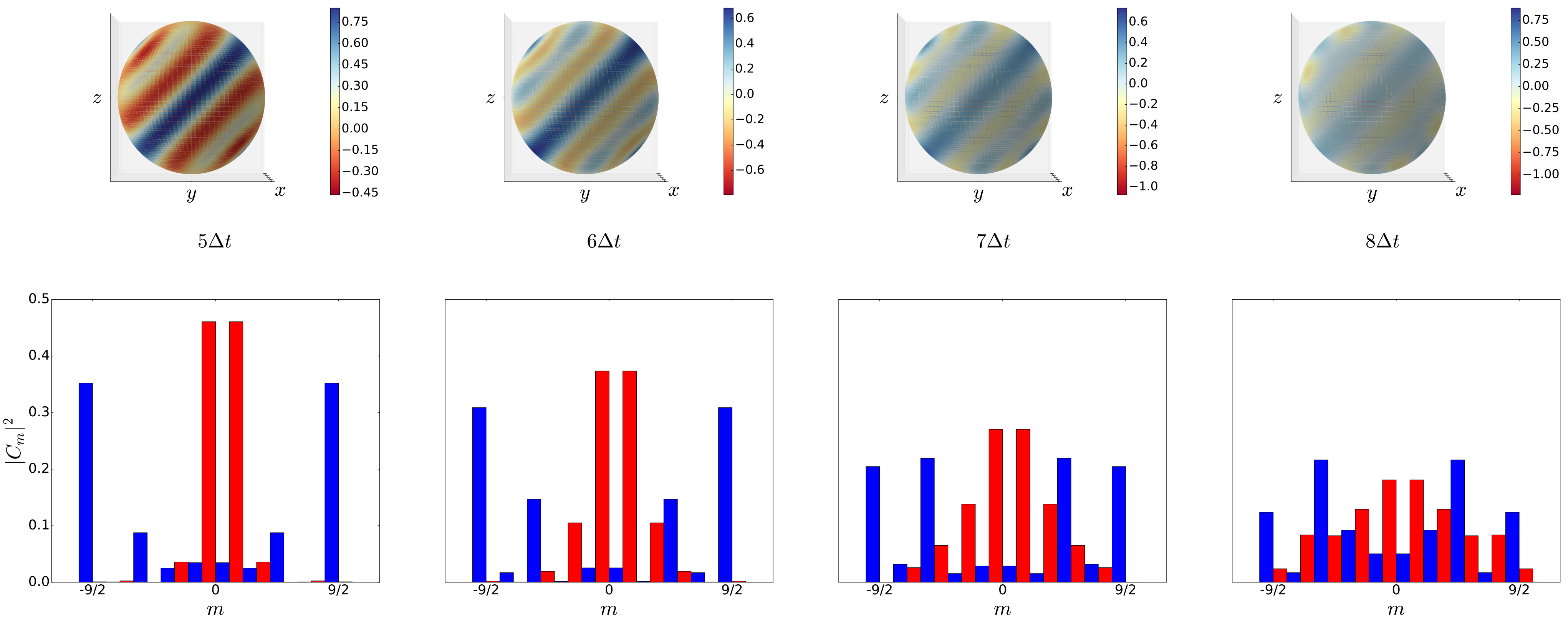

Anti-squeezing progression . . .

Dependence on Initial State Position

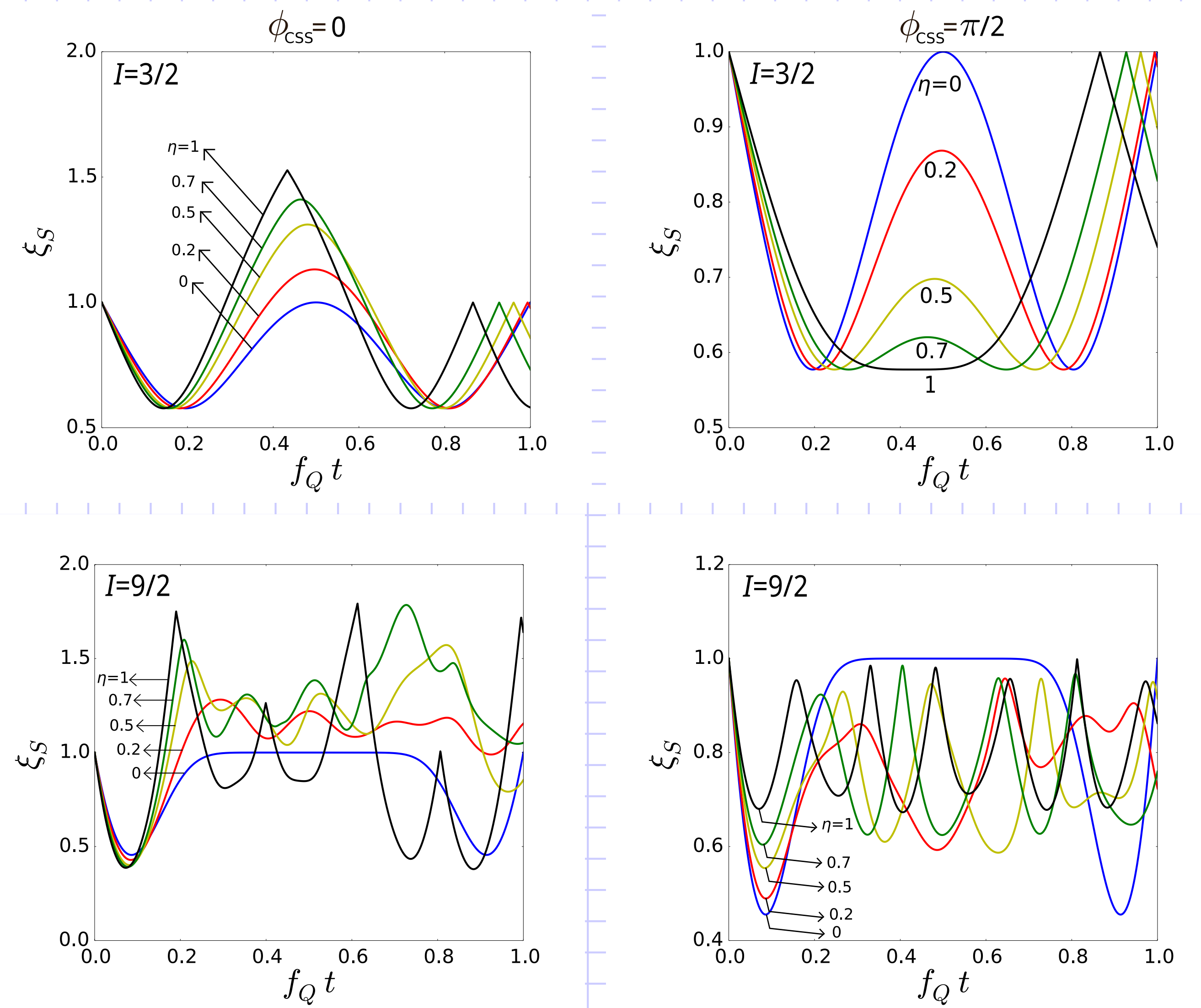

Y. Aksu Korkmaz and CB, Phys. Rev. A **93**, 013812 (2016)

Squeezing Rate

$$\mathcal{Q} = 2I\sqrt{\left[\eta\cos 2\varphi(1+\cos^2\vartheta) + 3\sin^2\vartheta\right]^2 + 4\eta^2\cos^2\vartheta\sin^2 2\varphi}$$

T. Opatrný, Phys. Rev. A **91**, 053826 (2015)

$I = 9/2,\ \eta = 0.5$

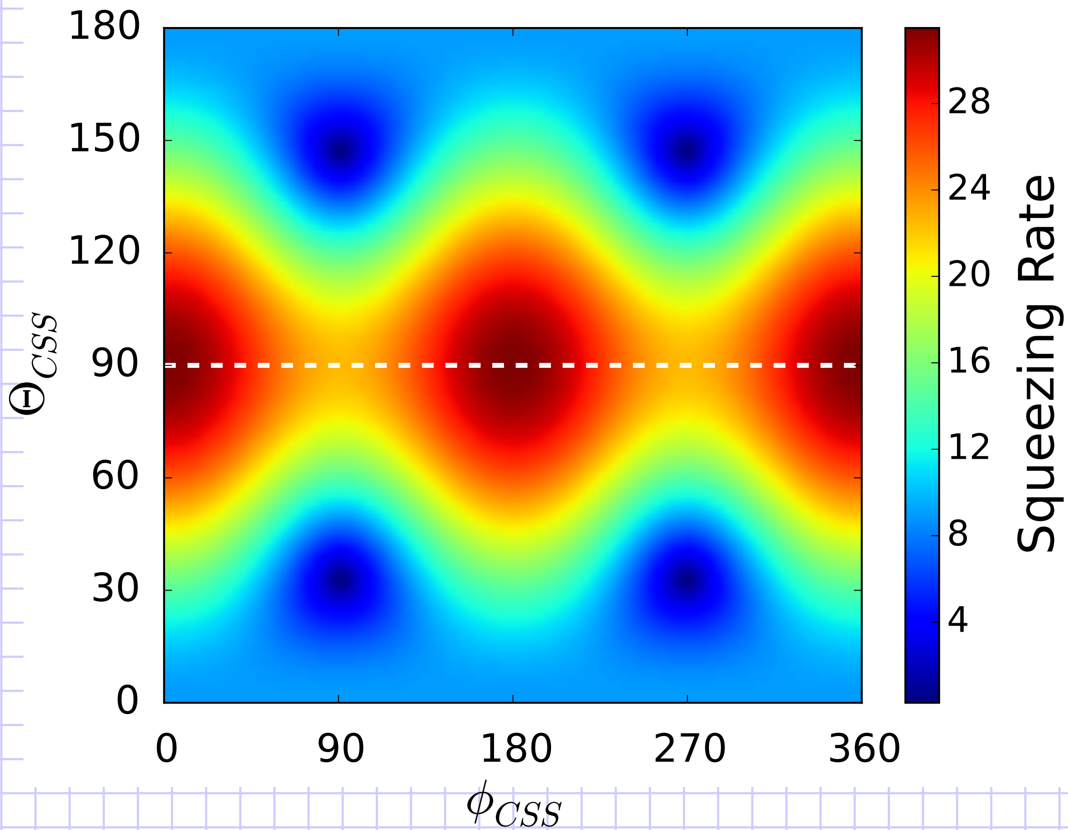

Y. Aksu Korkmaz and CB, Phys. Rev. A **93**, 013812 (2016)

Cat States: Generation & Stabilization

Cat States

- Macroscopically-distinguishable superposition of coherent states: $|\alpha\rangle$
- Applications: quantum metrology, fault-tolerant coding,...
- Even/Odd cat states: $\mathcal{N}\left[|\alpha\rangle + |-\alpha\rangle\right]$ and $\mathcal{N}\left[|\alpha\rangle - |-\alpha\rangle\right]$,
- Yurke-Stoller state: $\mathcal{N}\left[|\alpha\rangle \pm i\,|-\alpha\rangle\right]$

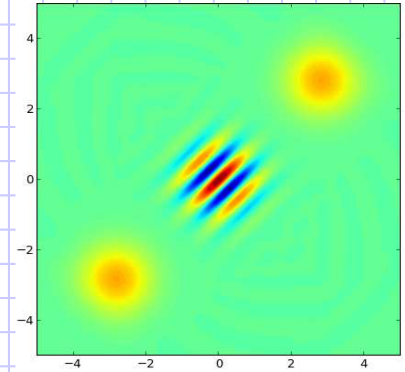

Source: QuTiP

Spin cat states over the Bloch sphere via Quadrupole Interaction

- Equator-bound spin cat state: $\left[|Y\rangle + e^{i\varphi}\,|-Y\rangle\right]$
- Polar-bound spin cat state: $\left[|Z\rangle + e^{i\varphi}\,|-Z\rangle\right]$
- The x-axis (the minor EFG) to serve as the key rotation direction

Cat States

- Macroscopically-distinguishable superposition of coherent states: $|\alpha\rangle$
- Applications: quantum metrology, fault-tolerant coding,...
- Even/Odd cat states: $\mathcal{N}\left[|\alpha\rangle + |-\alpha\rangle\right]$ and $\mathcal{N}\left[|\alpha\rangle - |-\alpha\rangle\right]$,
- Yurke-Stoller state: $\mathcal{N}\left[|\alpha\rangle \pm i\,|-\alpha\rangle\right]$

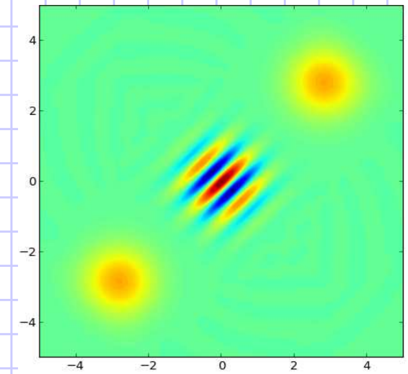

Source: QuTiP

Spin cat states over the Bloch sphere via Quadrupole Interaction

- Equator-bound spin cat state: $\left[|Y\rangle + e^{i\varphi}\,|-Y\rangle\right]$
- Polar-bound spin cat state: $\left[|Z\rangle + e^{i\varphi}\,|-Z\rangle\right]$
- The x-axis (the minor EFG) to serve as the key rotation direction
- But, how to break-away from quasi-periodic cycle, i.e., stabilization??

Phase Portraits

For a classical spin vector pointing toward the (θ, ϕ) direction,

$$H_\eta(\theta,\phi) = \frac{hf_Q I}{6}\left[3\cos^2\theta + \eta\sin^2\theta\cos 2\phi\right]$$

Hamilton EOM for the canonically conjugate variables $(\phi, P_\phi \equiv \cos\theta)$:

$$\begin{aligned}\dot{\phi} &= \frac{hf_Q I}{3} P_\phi\,(3-\eta\cos 2\phi) \\ \dot{P}_\phi &= \frac{hf_Q I}{3}\eta\left(1-P_\phi^2\right)\sin 2\phi\end{aligned}$$

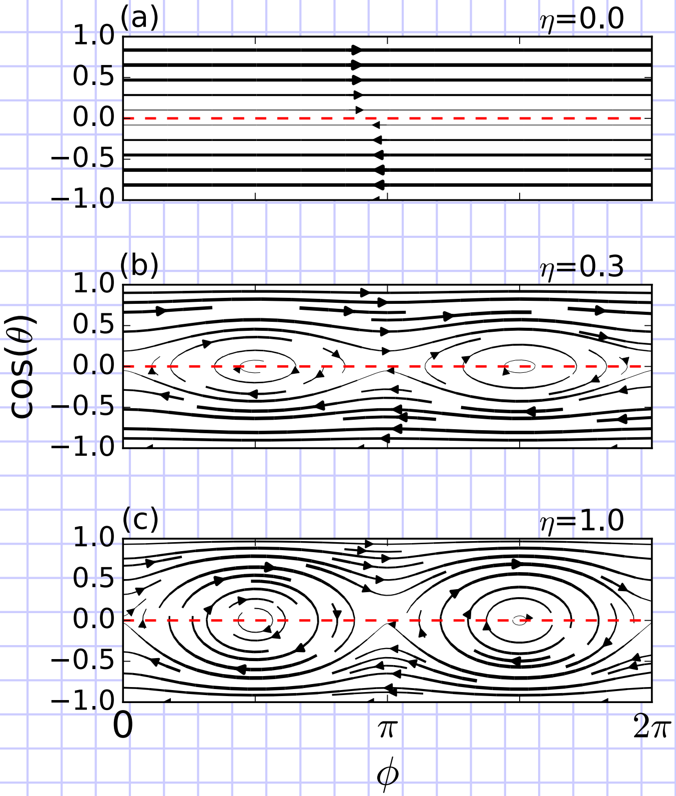

CB, arXiv:1610.07046 (2016)

Phase Portraits

For a classical spin vector pointing toward the (θ, ϕ) direction,

$$H_\eta(\theta, \phi) = \frac{hf_Q I}{6}\left[3\cos^2\theta + \eta\sin^2\theta\cos 2\phi\right]$$

Hamilton EOM for the canonically conjugate variables $(\phi, P_\phi \equiv \cos\theta)$:

$$\begin{aligned}\dot{\phi} &= \frac{hf_Q I}{3} P_\phi \left(3 - \eta\cos 2\phi\right) \\ \dot{P}_\phi &= \frac{hf_Q I}{3}\eta\left(1 - P_\phi^2\right)\sin 2\phi\end{aligned}$$

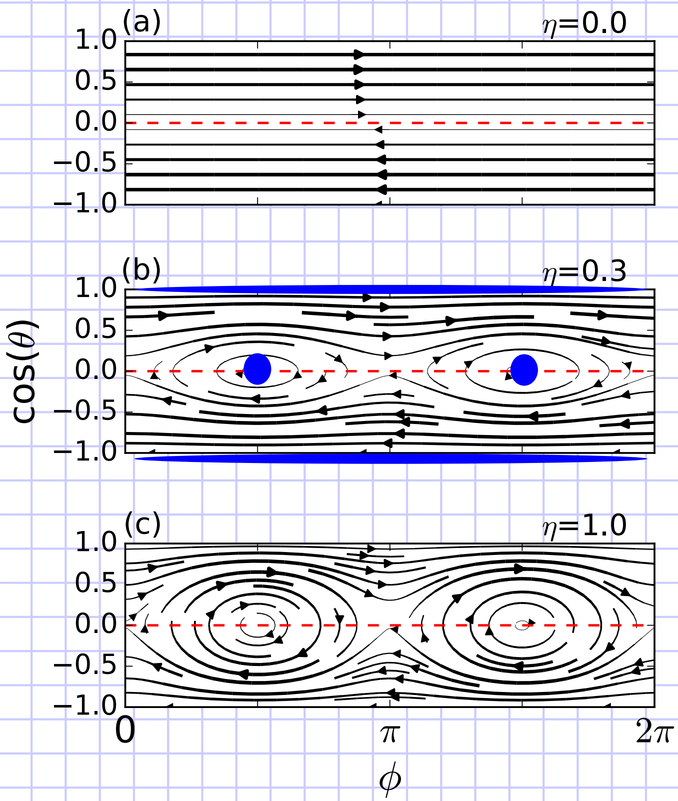

Four Fixed Points: $\pm Y$ and $\pm Z$ axes

CB, arXiv:1610.07046 (2016)

Measures

How close is generated state, $|\psi\rangle$ to a target state, $|\beta\rangle$?

- Fidelity: $|\langle\beta|\psi\rangle|$ (for pure states)
- QFI: $\mathcal{F}(\psi, \hat{A}) = 4\,\mathcal{V}_\psi(\hat{A})$, where, $\mathcal{V}_\psi(\hat{A}) = \langle\psi|\hat{A}^2|\psi\rangle - \langle\psi|\hat{A}|\psi\rangle^2$ is the variance
- Effective size for a spin I system (an absolute macroscopicity measure)
  $N_{\text{eff}}^{\text{F}}(\psi) = \max_{\hat{A}\in\mathcal{A}} \mathcal{F}(\psi, \hat{A})/(2I)$ (maximize over operators within the relevant set $\mathcal{A}$)
- Relative QFI: degree of *catness* of a superposed state $|\psi_S\rangle = (|\psi_a\rangle + |\psi_b\rangle)/\sqrt{2}$,

$$N_{\text{eff}}^{\text{rF}}(\psi_S) = \frac{N_{\text{eff}}^{\text{F}}(\psi_S)}{\left[N_{\text{eff}}^{\text{F}}(\psi_a) + N_{\text{eff}}^{\text{F}}(\psi_b)\right]/2}$$

- For pure states, and choosing as the relevant interferometric measurement operators the spin along directions u (i.e., $\hat{I}_u$)

$$N_{\text{eff}}^{\text{rF}}(\psi_S) = \frac{2\,\mathcal{V}_S(\hat{I}_S)}{\left[\mathcal{V}_a(\hat{I}_a) + \mathcal{V}_b(\hat{I}_b)\right]}$$

- $\mathcal{V}_{CSS} = I/2$, and $\mathcal{V}_{cat} = I^2$, Maximum $N_{\text{eff}}^{\text{rF}} \to 2I$
- Normalized rQFI: Catness of an evolving state ψ $\overline{N}_{\text{eff}}^{\text{rF}}(\psi) = \frac{\mathcal{V}_\psi(\hat{I}_S)}{I^2}$, ranges between 0 to 1.

Basic Operation

$I = 5/2,\ \eta = 1$

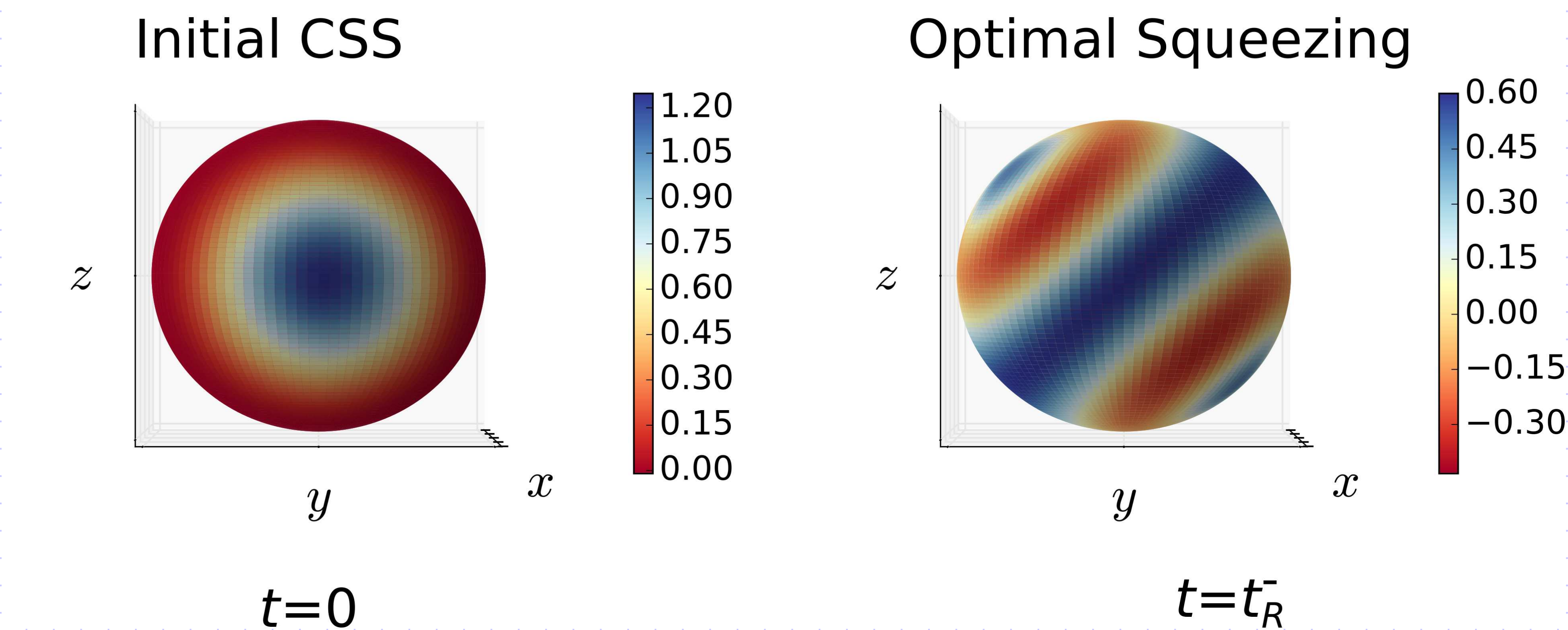

CB, arXiv:1610.07046 (2016)

Basic Operation

$I = 5/2,\ \eta = 1$ Target state: $[|Z\rangle + e^{i\varphi}|-Z\rangle]$

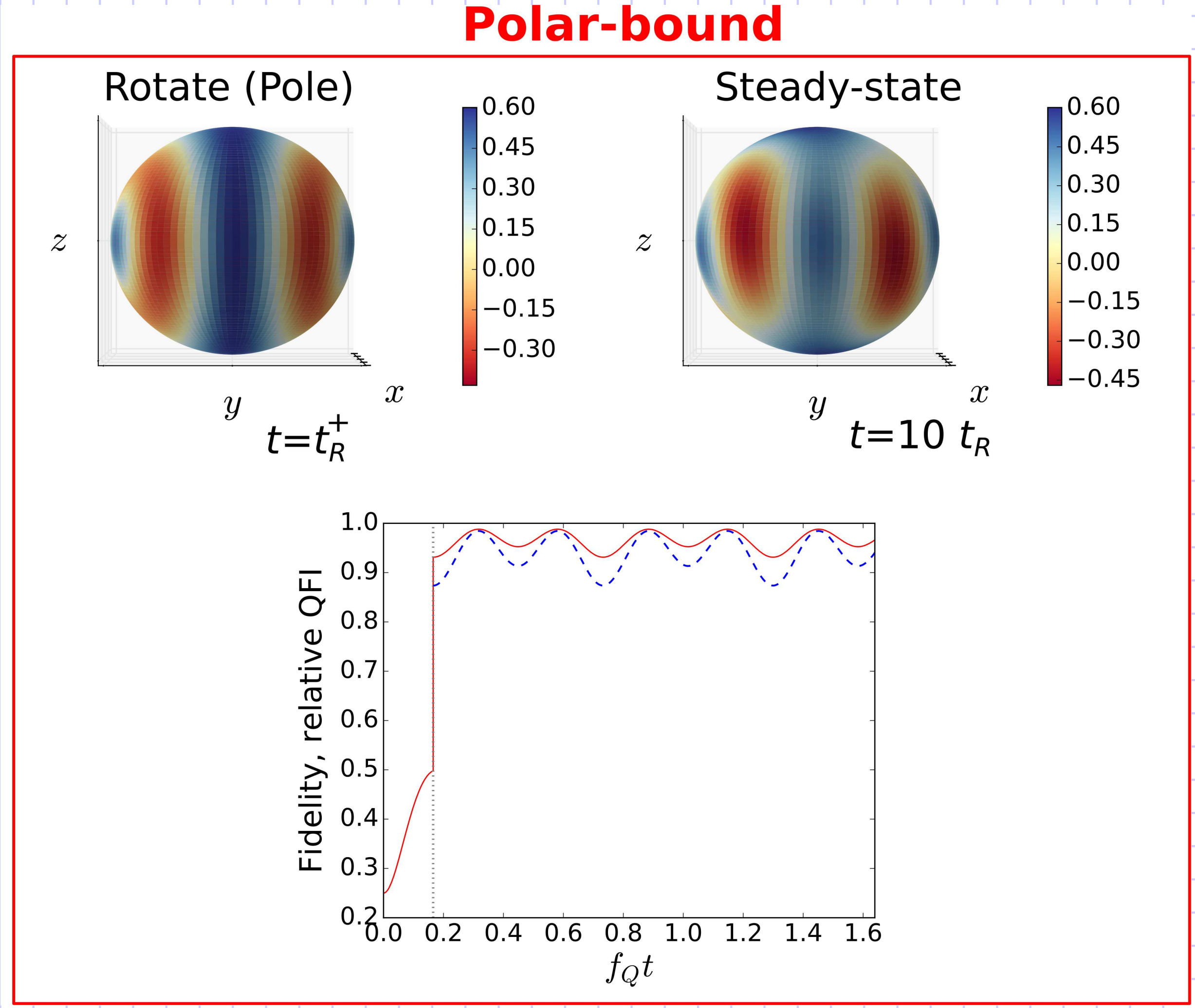

CB, arXiv:1610.07046 (2016)

Basic Operation

$I = 5/2$, $\eta = 1$ Target state: $[|Y\rangle + e^{i\varphi}|-Y\rangle]$

Equator-bound

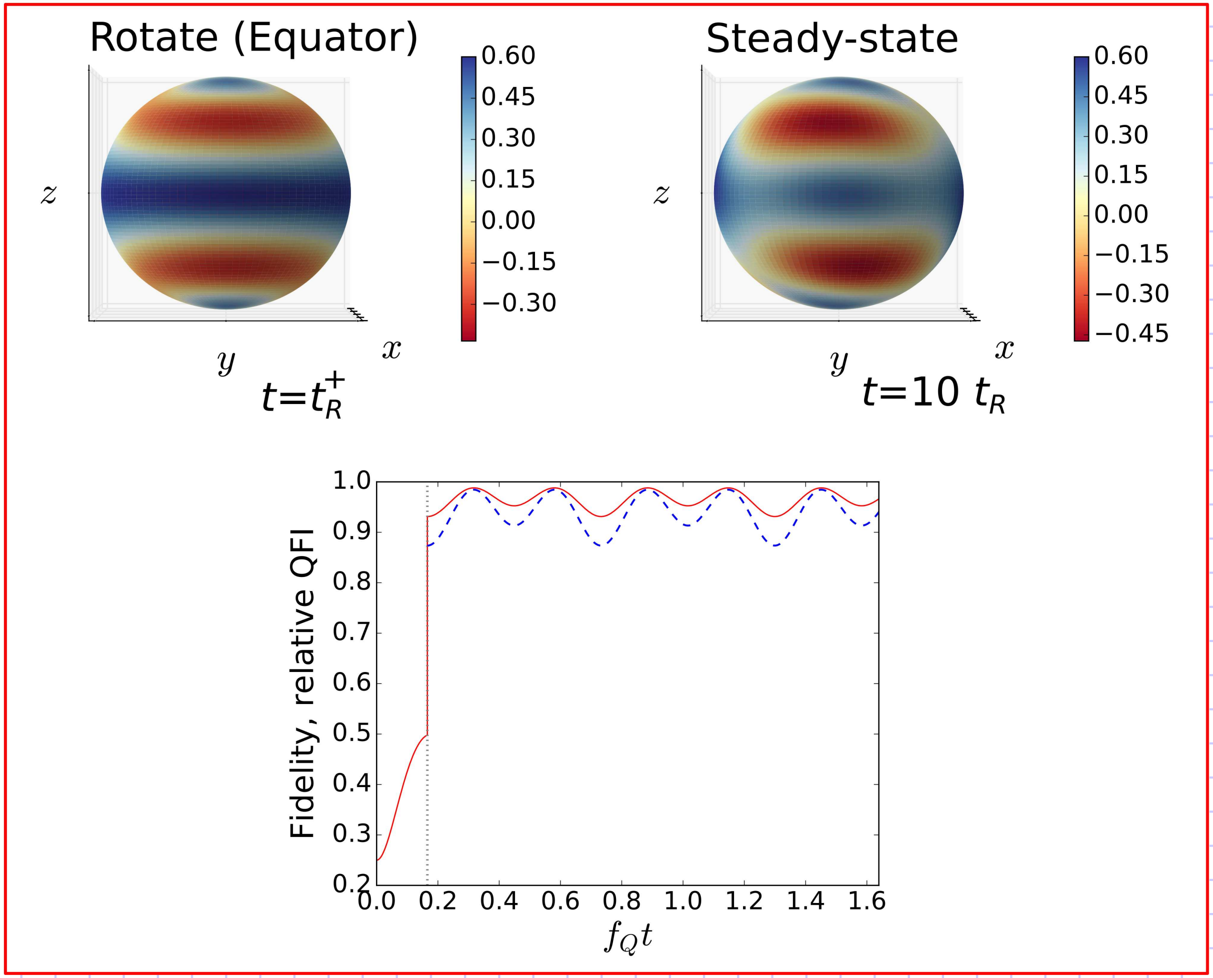

CB, arXiv:1610.07046 (2016)

Optimal Parameters

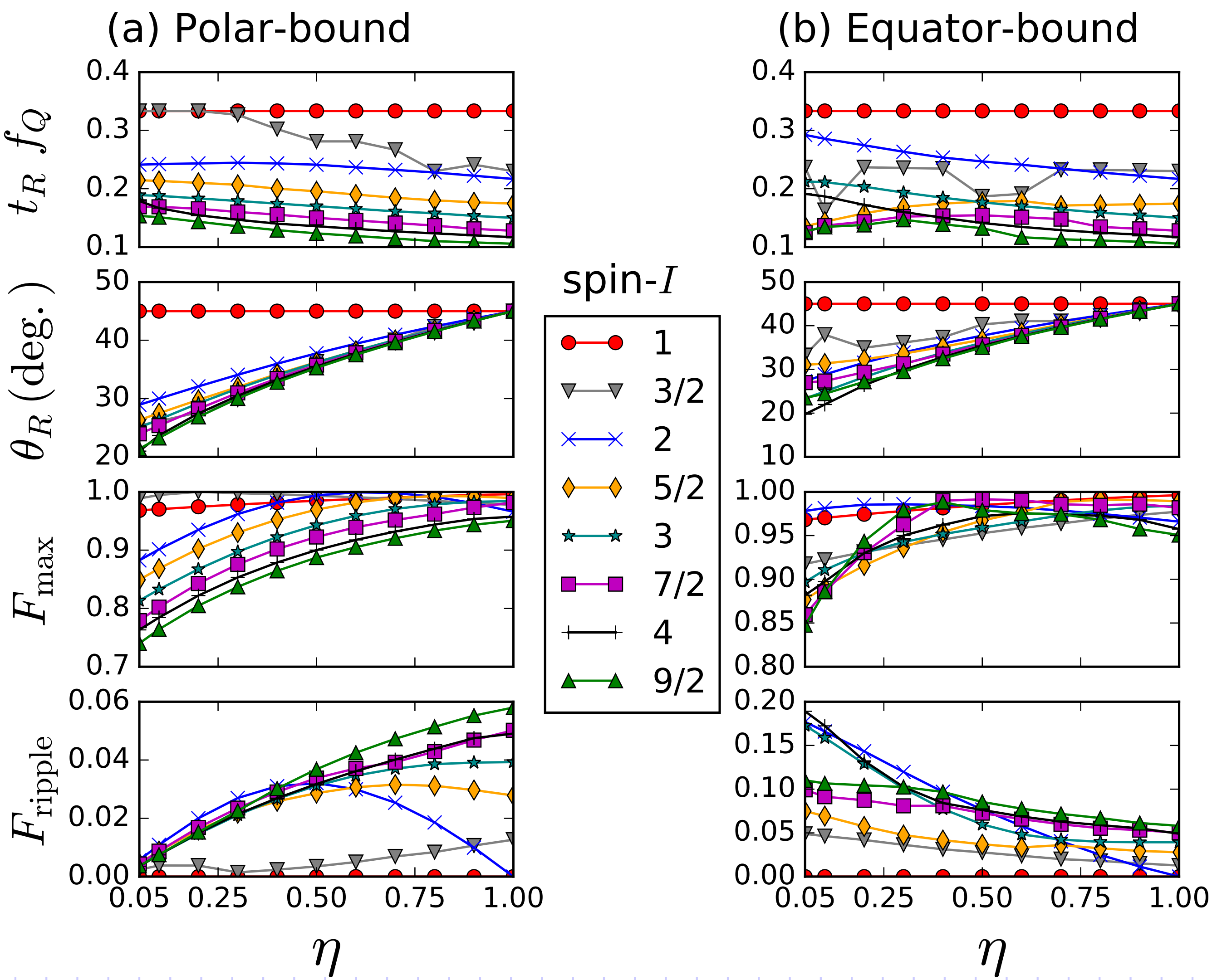

CB, arXiv:1610.07046 (2016)

Sensitivity to Parameters

Deviations from Optima: 5% (Dashed), 10% (Dotted)

Equator-Bound: $I = 3/2$, $\eta = 0.3$

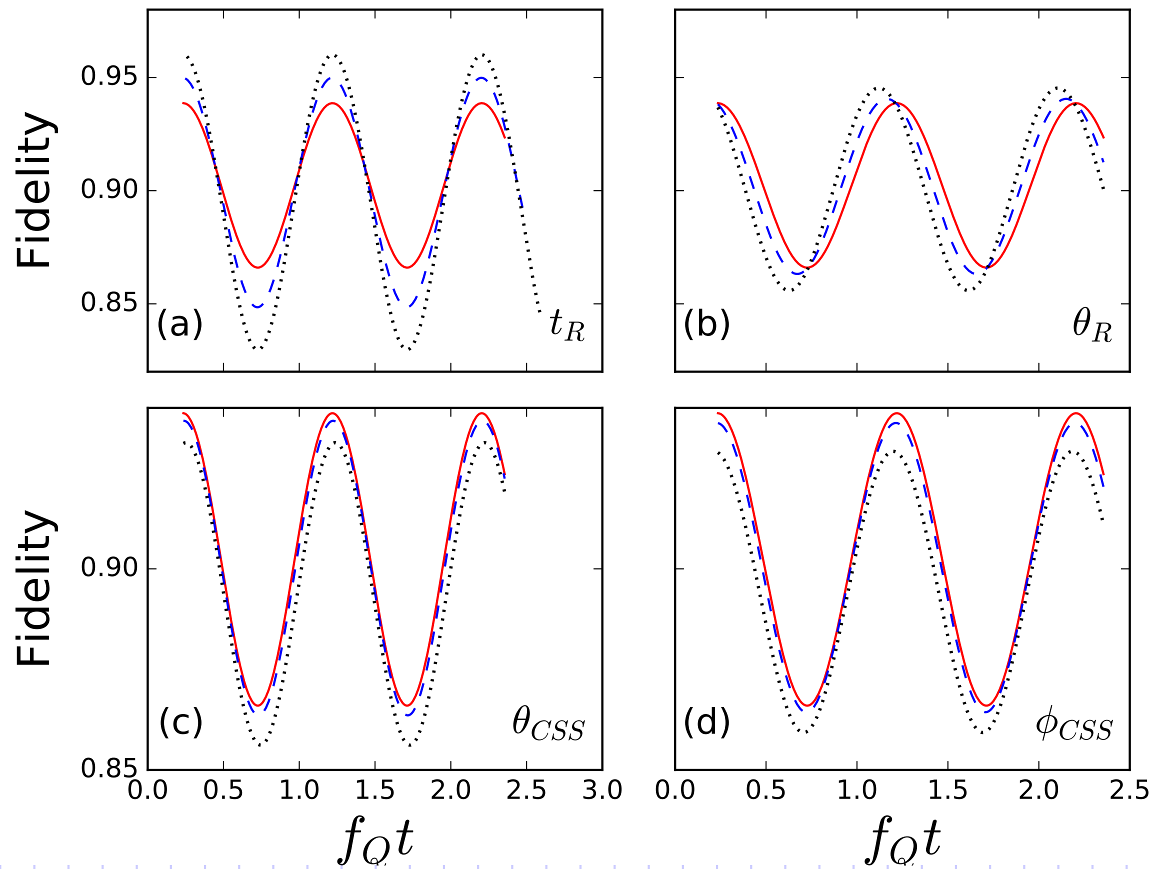

CB, arXiv:1610.07046 (2016)

Sensitivity to Parameters

Deviations from Optima: 5% (Dashed), 10% (Dotted)

Polar-Bound: $I = 3/2$, $\eta = 0.3$

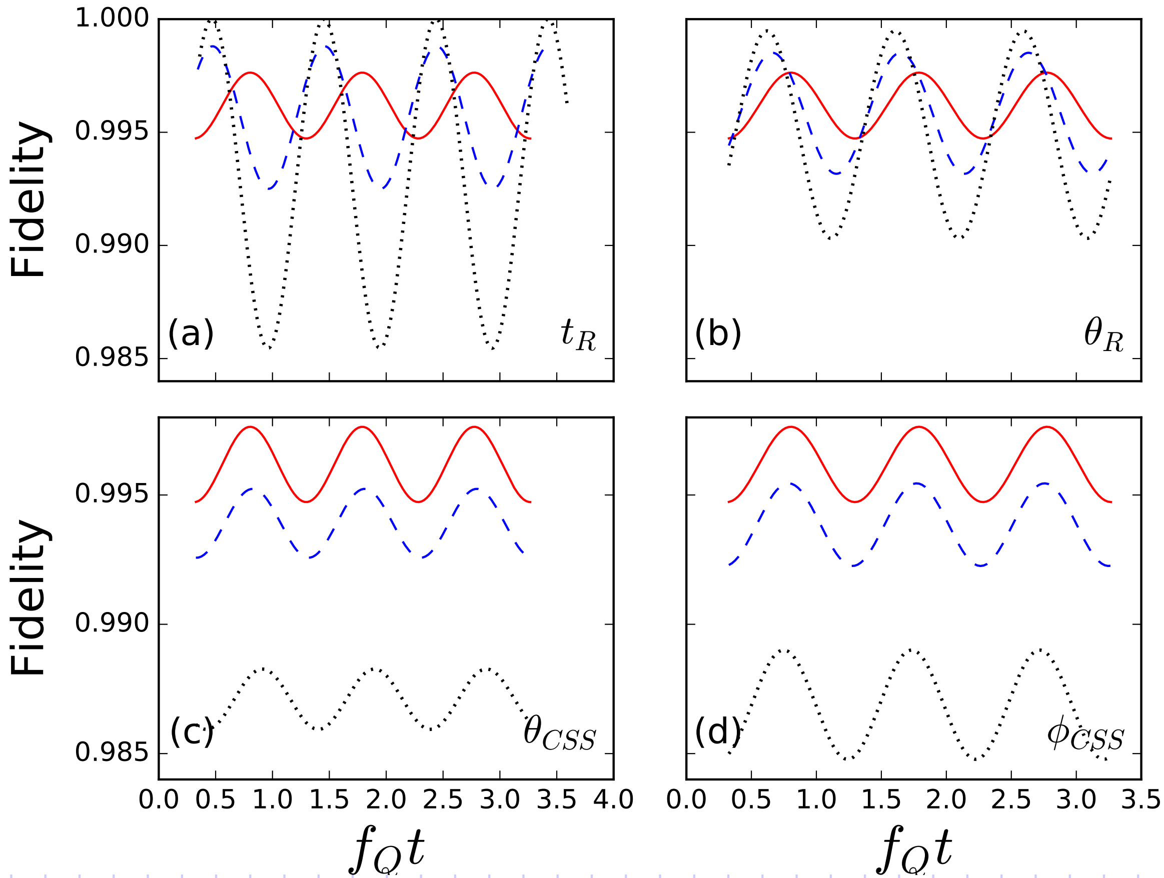

CB, arXiv:1610.07046 (2016)

Timescales & Decoherence

Order of Magnitudes

- Fundamental time scale in QI, f_Q governed by strain
  - Self-assembled quantum dots (SAQD), f_Q ~2–8 MHz
  - Nitrogen vacancy (NV) defect centers, f_Q ~10 MHz
  - Single-crystal $KClO_3$, $f_Q = 28.1$ MHz
- In the absence of hyperfine coupling to the confined electronic spin: Primary decoherence process, phase damping
  - SAQD: ^{69,71}Ga, ^{75}As, ^{115}In nuclei, $T_2 = 1/\gamma$ ~1–5 ms
  - NV: ^{14}N nucleus, T_2 ~1 ms
  - $KClO_3$: ^{35}Cl nucleus, $T_2 = 4.6$ ms
- Markedly distinct systems, $f_Q/\gamma = f_Q T_2 \sim 10^3 - 10^5$

$\Longrightarrow$ Strong quadrupolar coupling regime

Decoherence: phase-flip channel

- Cat states particularly vulnerable to phase noise
- Lindblad Master equation

$$\frac{\mathrm{d}}{\mathrm{d}t}\hat{\rho}_S(t) = -\frac{i}{\hbar}\left[\hat{H}, \hat{\rho}_S(t)\right] + \sum_{m=1}^{2I}\left[\hat{L}_m\hat{\rho}_S(t)\hat{L}_m^\dagger - \frac{1}{2}\left\{\hat{L}_m^\dagger\hat{L}_m, \hat{\rho}_S(t)\right\}\right]$$

- Lindblad operators:

$$\hat{L}_m = \sqrt{\binom{2I}{m}\left(\frac{1-e^{-\gamma}}{2}\right)^m\left(\frac{1+e^{-\gamma}}{2}\right)^{2I-m}}\,\hat{I}_z^m$$

where $\gamma = 1/T_2$ is the dephasing rate

S. Pirandola et al. Phys. Rev. A 77, 032309 (2008)

Effect of Decoherence

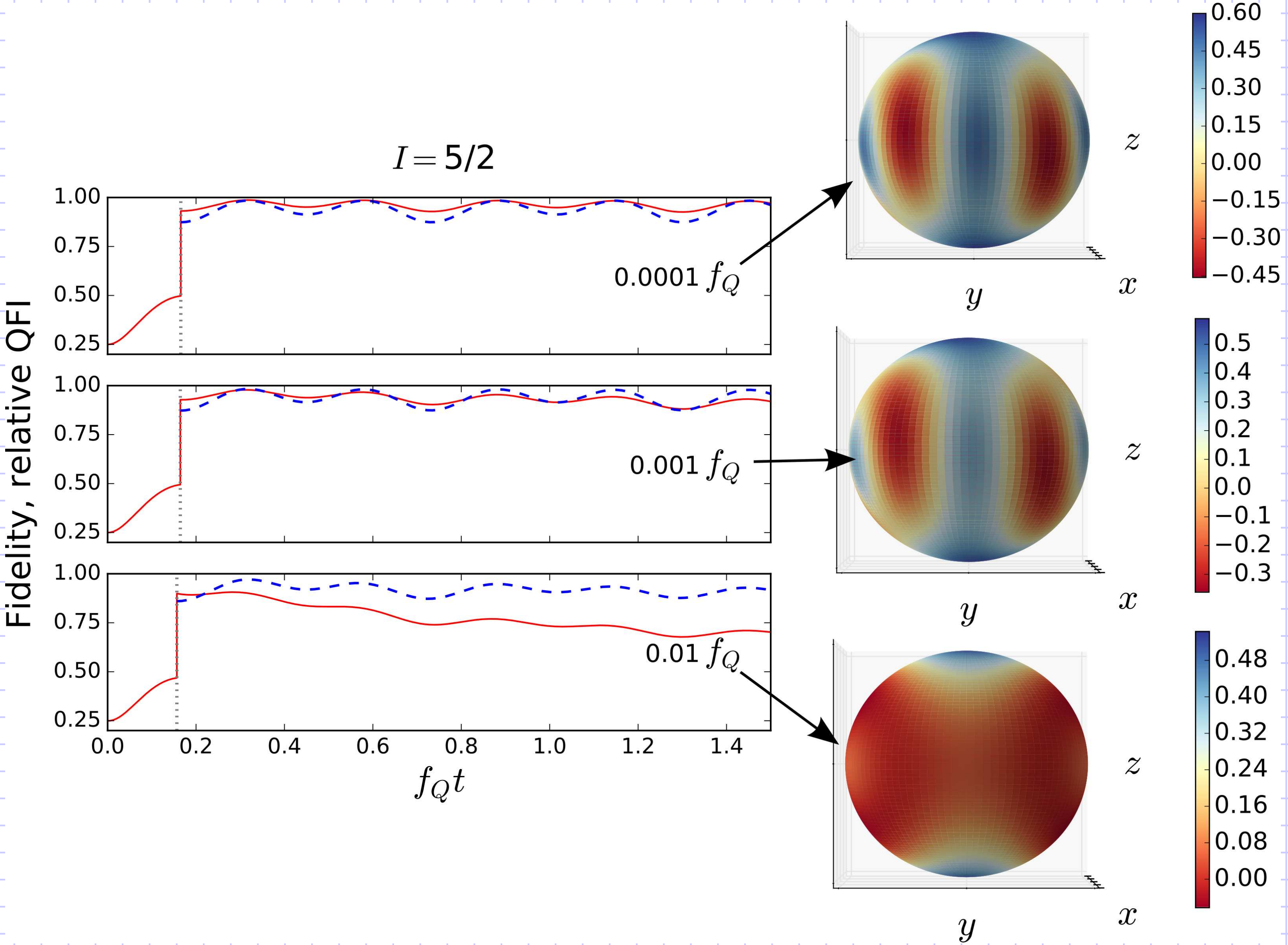

CB, arXiv:1610.07046 (2016)

Mod 4 Spin Cat States

- Macroscopically-distinguishable superposition of 4 spin cat states e.g. $[(|Z\rangle + |-Z\rangle) - (|Y\rangle + i|-Y\rangle)]$
- Generate with a 3-pulse scheme:
  - [Pulse-1] Produce a mod 2 cat state (say, $|Z\rangle + |-Z\rangle$)
  - [Pulse-2] Rotate by $\pi/2$ back to x-axis $\Longrightarrow$ $[|X\rangle + |-X\rangle]$
  - Evolve these antipodal CSSs under $\hat{H}_\eta$: countertwisted squeezing
  - [Pulse-3] Rotate around x-axis (optimized in time/angle) to split and place one of them to the poles and the other to $\pm y$-axes
- Rotating spin cat state superposed to a fixed counterpart: $[(|Z\rangle + |-Z\rangle) + e^{i\omega_2 t}(|Y\rangle + i|-Y\rangle)]$
  Enables a relative phase accumulation
- Crucial in cat codes to protect against bit flips
  [Ofek et al. Nature **536**, 441 (2016)]

Decoherence on mod 4 Cat States

$I = 5/2$, $\eta = 1$, No decoherence

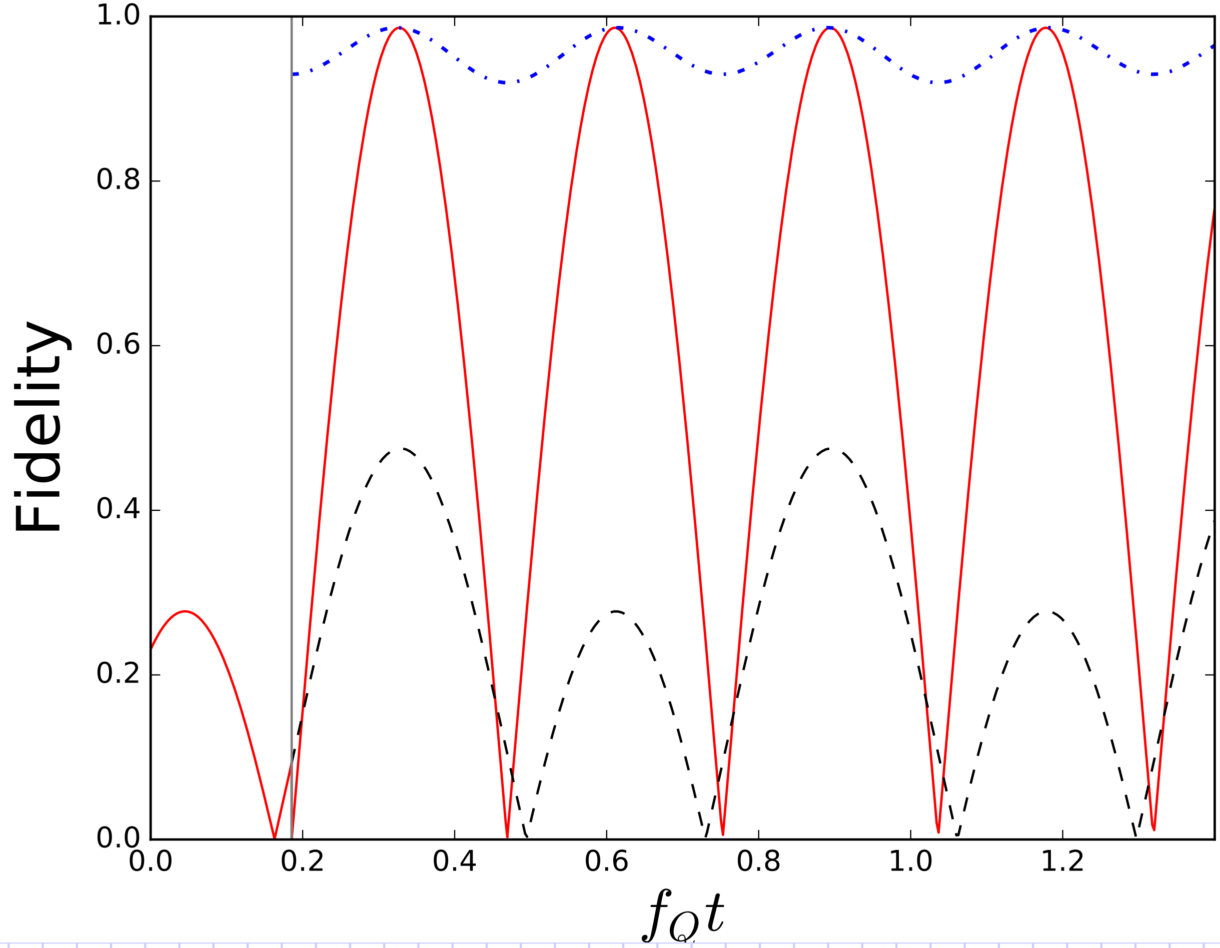

CB, arXiv:1610.07046 (2016)

Decoherence on mod 4 Cat States

$I = 5/2$, $\eta = 1$, $\gamma = 10^{-4} f_Q$

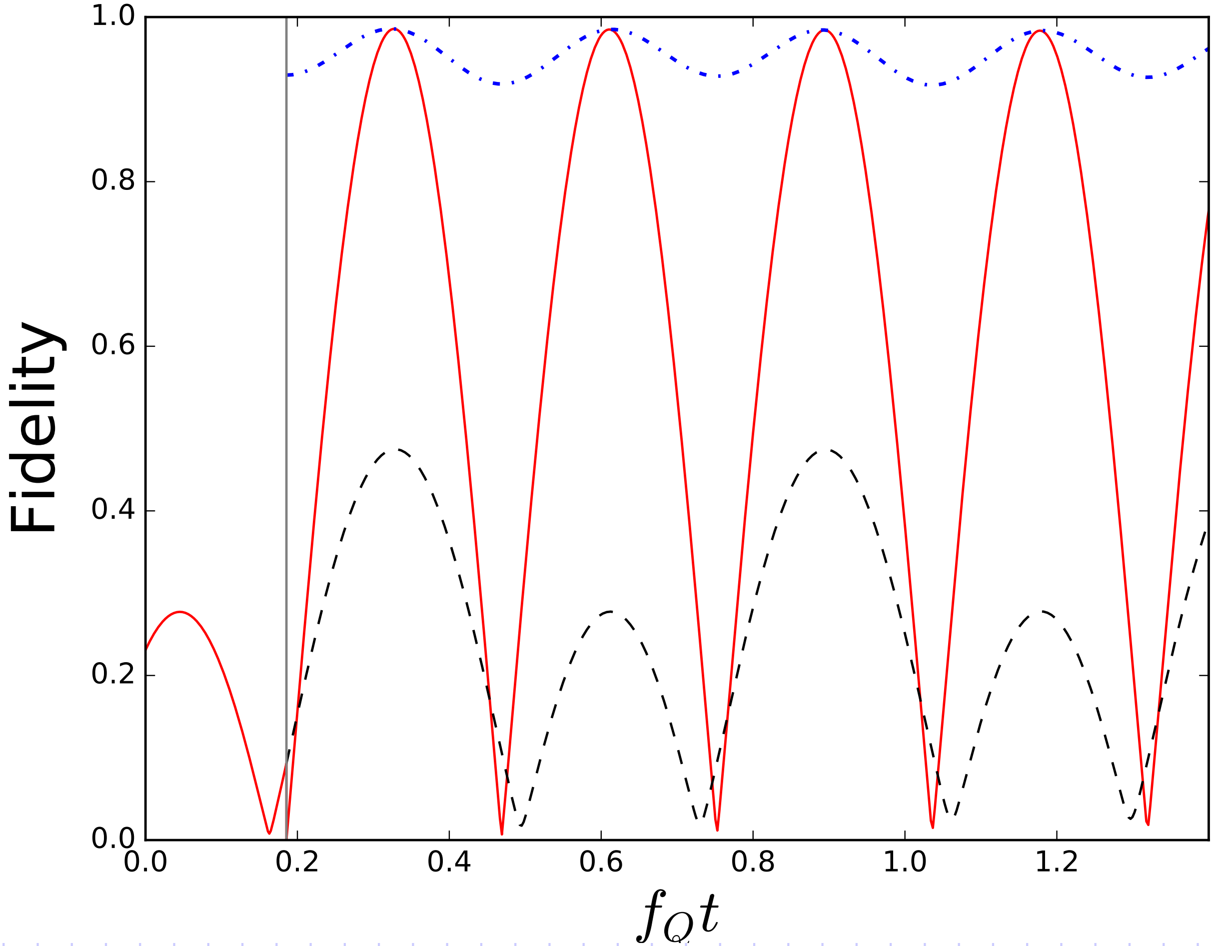

CB, arXiv:1610.07046 (2016)

Decoherence on mod 4 Cat States

$I = 5/2$, $\eta = 1$, $\gamma = 10^{-2} f_Q$

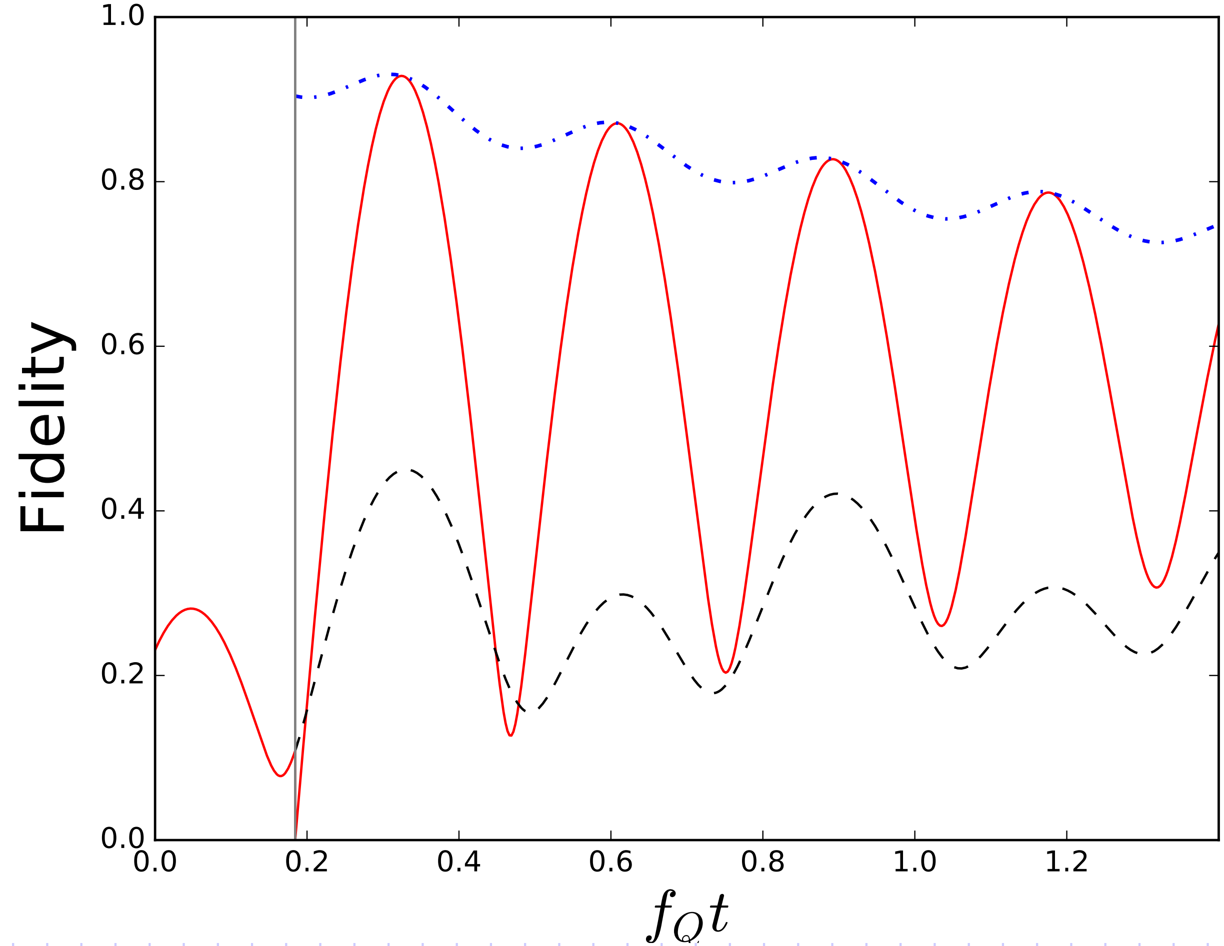

CB, arXiv:1610.07046 (2016)

Scaling of Cat State Decoherence with I

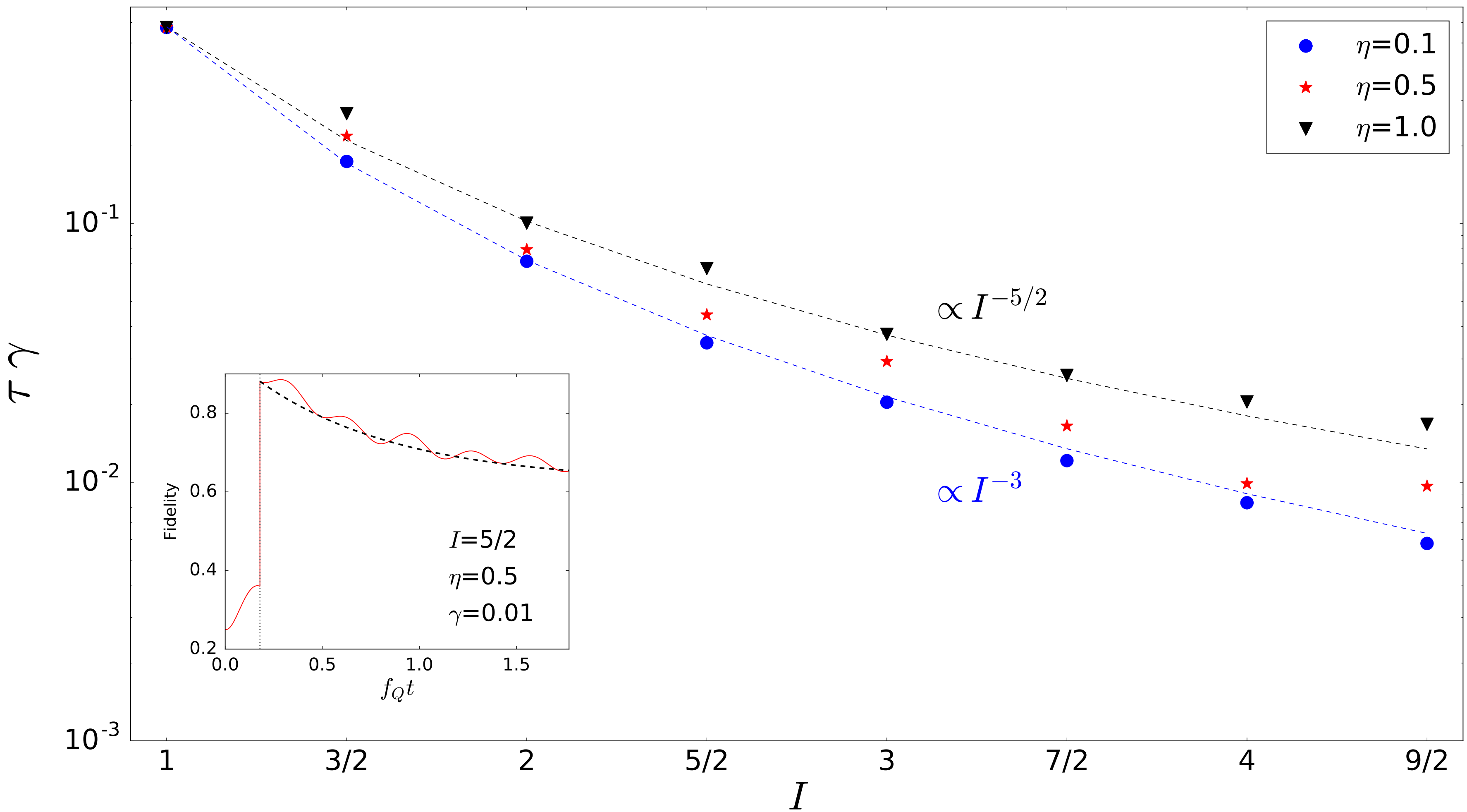

CB, arXiv:1610.07046 (2016)

Discussion: Practical Context

- Nuclear spin with $I \geq 1 \implies$ a small-scale quantum info processor
  Permutation parity: Z. Gedik et al. Sci. Rep. **5**, 14671 (2015)
- Quantum memory protection through parity detection w/o leaking out the stored quantum info: N. Ofek et al. Nature **536**, 441 (2016)
- In quantum sensing, surpassing standard quantum limit via cat states

- BEC:
  - N-atom entanglement $\implies$ spin-$N/2$ collective Hilbert space
  - Exceedingly more fragile to decoherence as N grows
- Quadrupolar Nucleus:
  - No entanglement (pure state of a *single* nuclear spin)
  - Less fragile to decoherence (I is inherently capped)

Conclusions

- Generating stabilized nuclear spin cat states via biaxial QI
- Mod 2 cat states attain fidelities around 0.95
- Robust under variations in the parameters
- Mod 4 cat with one of its constituent mod 2 cats rotating wrt EFG axes
- Utilized in cat codes to protect against bit flips
- Phase-noise-tolerant within currently accessible decoherence levels

Conclusions

- Generating stabilized nuclear spin cat states via biaxial QI
- Mod 2 cat states attain fidelities around 0.95
- Robust under variations in the parameters
- Mod 4 cat with one of its constituent mod 2 cats rotating wrt EFG axes
- Utilized in cat codes to protect against bit flips
- Phase-noise-tolerant within currently accessible decoherence levels

İlginiz için teşekkürler

Thank you for your attention